Desalination and Water Treatment
www.deswater.com

doi: 10.5004/dwt.2017.21269

90 (2017) 23–31
September

Comparison of pretreatment methods for wastewater reclamation and seawater desalination in forward osmosis process

Younghoon Ko, Yongjun Choi, Jaeseok Ju, Youngsun Jang, Sangho Lee*

School of Civil and Environmental Engineering, Kookmin University, Jeongneung-Dong, Seongbuk-Gu, Seoul, Korea, Tel. +82 2 910 4529; Fax: +82 2 910 4939; email: sanghlee@kookmin.ac.kr (S. Lee)

Received 4 February 2017; Accepted 29 July 2017

ABSTRACT

Forward osmosis (FO) has drawn attention as an emerging technology for seawater desalination and wastewater treatment/reuse. Nevertheless, little information is available on the selection of proper pretreatment for FO process. Accordingly, this study focused on the comparison of different pretreatment methods for FO to provide into the selection of its pretreatments. Two groups of pretreatment methods were compared: membrane-based pretreatments including microfiltration and ultrafiltration and conventional filtration using activated filter media. Experiments were conducted to explore correlations between the silt density index/modified fouling index and FO flux decline. The Hermia's model equations were applied to analyze the results and to identify the dominant fouling mechanisms. The possibility of using a fouling index to predict FO fouling was also examined.

Keywords: Pretreatment; Forward osmosis; Hermia's model; Membrane; Fouling; Fouling index

1. Introduction

With an increase in water demands and a decrease in water supplies, desalination has become an important source of freshwater [1,2]. Membranes such as microfiltration, ultrafiltration, and reverse osmosis (RO) are considered to be highly competitive and promising candidates for water resource development and desalination [3–6]. Currently, the most economical and popular desalination technology is RO mainly due to advancements in membrane technology [2]. However, RO still faces three key obstacles: membrane fouling, high energy consumption, and limited water recovery [7]. These problems of RO make FO become increasingly attractive, especially in desalination [8].

Recently, there is a growing interest in novel membrane technologies such as forward osmosis (FO). FO is an osmotic process that uses a semi-permeable membrane to separate water from dissolved solutes by an osmotic pressure gradient. Unlike RO, FO does not require high pressure for separation. Accordingly, FO has been considered as an emerging technology for water reuse [9–11] and seawater desalination [12–15]. Moreover, FO can be also used for power generation using salinity gradients, which is called as pressure retarded osmosis (PRO) [16–20].

However, membrane systems inherently have problems associated with fouling [21,22]. Although it has been reported that FO fouling is less severe than RO fouling, it does not imply that there is no fouling in FO. Since FO is applied not only for seawater desalination but also for wastewater reclamation, the feed water for FO may have higher fouling propensity. Accordingly, proper pretreatment is critical for mitigating fouling of FO process.

There are two major objectives in this study: (1)the comparison of fouling tendencies for FO membranes. We used two different FO membranes and applied various pretreatment techniques to examine the fouling properties; (2) the application of SDI and MFI to predict fouling potential of FO membranes. We investigated the correlation between SDI/MFI and flux reduction rate and attempted to interpret the results based on the proposed fouling mechanism. The final objective is the application of fouling index that has better ability to predict fouling potential in FO systems.

* Corresponding author.

Presented at the 9th International Desalination Workshop: Sustainable Desalination (IDW 2016), 13–15 November 2016, Abu Dhabi, UAE.

2. Materials and methods

2.1. Source water of feed and draw solution

Wastewater from Korean steelworks was used as the feed water for FO experiments. Seawater from the southern coast in Korea was used as the draw solution. The water quality parameters for the wastewater and seawater are summarized in Tables 1 and 2, respectively.

2.2. Pretreatment methods

2.2.1. Membrane pretreatment system

Two types of pretreatment methods were compared. One of them is membrane-based pretreatment including microfiltration (MF) and ultrafiltration (UF). A schematic diagram of the pretreatment device of flat membrane in laboratory-scale is shown in Fig. 1. Three different membranes were compared in this study, including a cartridge filter (CF) with the nominal pore size of 5 microns, a MF membrane with the nominal pore size of 0.22 micron, and an UF membrane with the molecular weight cut-off of 100 kDa. Each experiment was carried out using commercially available polymeric membranes. Both CF and MF membranes were obtained from Merck Millipore Ltd. (Ireland), which were made of polycarbonate and polyethersulfone, respectively. UF membranes, made of polyethersulfone, were purchased from EMD Millipore Corporation (USA). Each pretreatment process was operated at a constant pressure. The CF and MF were operated in the range of 0.01–0.10 bar, and the UF was operated in the range of 0.10–1.5 bar.

2.2.2. AFM pretreatment system

A media filter was also applied as the pretreatment for FO. Activated filter media (AFM) prepared by recycling green glass bottles was used as filter media. A schematic diagram of the pretreatment device of AFM in lab scale is shown in Fig. 2.

Table 1
The wastewater quality parameters

Category	Effluent
pH	8.46
TOC (mg/L)	5.87
UV_{254} (cm^{-1})	0.208
SS (mg/L)	12
Turbidity (NTU)	4.81
Conductivity (mS/cm)	4.43

Table 2
The seawater quality parameters

pH	8.14	TN (μg/L)	277
DO (mg/L)	8.09	TP (μg/L)	25.4
COD (mg/L)	1.08	Si as SiO_2 (μg/L)	127.2
SS (mg/L)	11.89	UV_{254} (cm^{-1})	0.021
Turbidity (NTU)	0.39	Chl-a (μg/L)	2.54
Conductivity (mS/cm)	46.4	Transparency	2.5

The tests were conducted either without or with the use of coagulant. The coagulant used in this study was polyaluminum chloride that had the Al_2O_3 content of 17%. The feed volume was 45 L and the operation linear velocity was maintained at 6 m/h. The AFM is classified into four types according to the degree of disassembly. The media of Grade "1" were used in this experiment. The details are shown in Table 3.

2.3. Experiments of SDI/MFI

Both SDI and MFI were measured according to the standard ASTM (American Society for Testing and Materials) method. Membrane filters (GE Healthcare Life Sciences, UK) made up of mixed cellulose ester with the pore size of 0.45 μm were used. During SDI tests, time required to pass a 500 mL feed through the filter was measured at 15 min intervals to provide filter clogging due to particle deposition on the membrane surface and cake filtration control of the permeate flux [23]. The decay in flow rate and/or permeate flux was converted to an SDI index number whose value should be between about 0 and 7. High levels of colloid and particle contamination were exhibited by fast membrane plugging and corresponding high SDI index values. The SDI value was calculated by measuring the time (min) for collecting the initial 500 mL (t_i) and the final

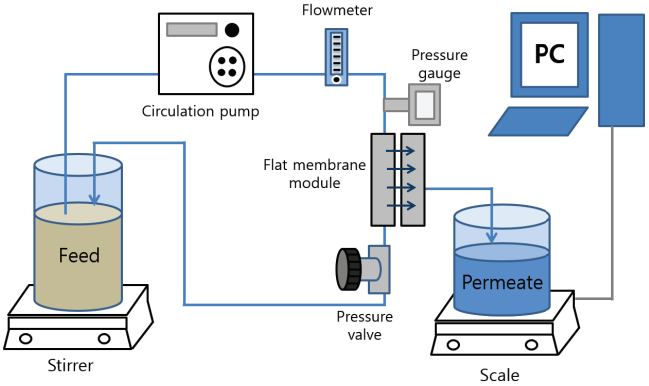

Fig. 1. Laboratory-scale pretreatment device of a flat membrane.

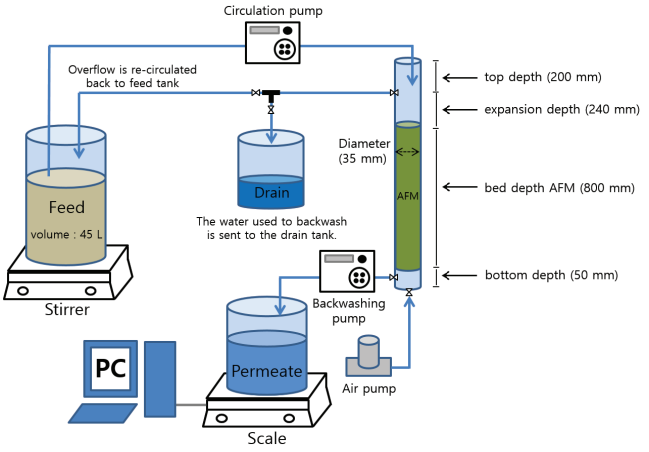

Fig. 2. Laboratory-scale pretreatment device of activated filter media.

Table 3
Sort of activated filter media

Specification	Grade "0"	Grade "1"	Grade "2"	Grade "3"
Particle size	250–500 μm	0.4–1 mm	1.0–2.0 mm	2.0–4.0 mm
Effective size	320 μm	0.46 mm	1.3 mm	2.6 mm
Hardness, mohs	>7	>7	>7	>7
Sphericity	>0.7	>0.7	>0.7	>0.7
Uniformity coefficient	1.5–1.7	1.5–1.7	1.5–1.7	1.5–1.7
Aspect ratio	2–2.4	2–2.4	2–2.4	2–2.4
Purity, %	>99.95	>99.95	>99.95	>99.95
Color, % green	>99	>99	>99	>99
Specific gravity (grain), kg/L	2.4	2.4	2.4	2.4
Embodied energy, kW/t	<72	<65	<50	<50
Bulk bed density, kg/L	1.28	1.25	1.23	1.22

500 mL (t_f) using Eq. (1). The third time interval (t_T) is 15 min and is the time between the collection of the initial and final sample. The MFI is defined by the slope of t/V vs. V under constant pressure filtration as shown in Eq. (2) [24,25], where μ, I, ΔP and A were the solution viscosity (Pa S), the fouling index, the applied pressure (Pa) and the membrane surface (m^2) area, respectively [25]. The fouling index, I, is the product of the specific cake resistance (α) and the foulant concentration (C_b, express to ppm). Accordingly, the MFI can increase due to an increase in not only organic deposition but also specific cake resistance by the formation of a more compact fouling layer, which is caused by the formation of intermolecular complexation of organic matter with calcium ions [25].

$$\mathrm{SDI}_T = \left(1 - \frac{t_i}{t_f}\right) \times \frac{100}{t_T} \quad (1)$$

$$\mathrm{MFI} = \frac{\mu I}{2\Delta P A^2} \quad (2)$$

$$I = \alpha \times C_b \quad (3)$$

2.4. Forward osmosis system

FO experiments were carried out using two different commercial FO membranes. Detailed information on these membranes was not provided by the membrane manufacturers. The feed and draw volumes were 2 L. For both membranes, the operating temperature was 21.5°C and flow rate was 0.3 L/min. The effective area of the FO membranes was 12.00 cm^2. A schematic diagram of FO device in laboratory scale is illustrated in Fig. 3.

2.5. Analytical methods

The total organic carbon (TOC) was measured using a TOC analyzer (DC-180, Rosemount, USA). The analysis of TOC was commissioned by a specialized agency in Korea (Korea Institute of Civil Engineering and Building Technology). The total dissolved solids (TDS) were analyzed by the digital precision meter (Multi 3420, Wissenschaftlich-Technische Werkstätten GmbH, Germany). The ultraviolet absorbance at 254 nm (UV254) was analyzed by DR/4000 UV–VIS spectrophotometer (HACH Company, USA). The turbidity was analyzed by handheld turbidimeter (Turb 430 IR, Wissenschaftlich-Technische Werkstätten GmbH, Germany). Each water quality analysis proceeded immediately at the end of experiment test.

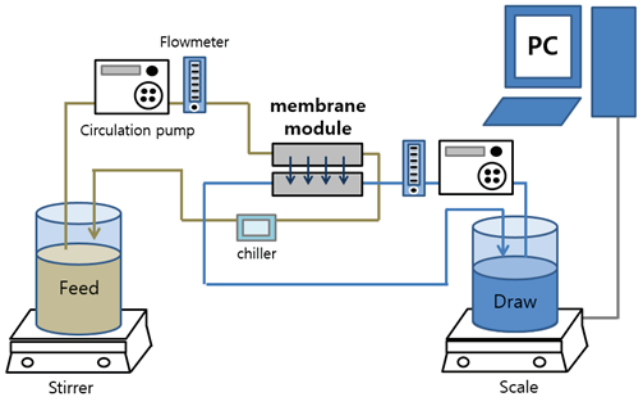

Fig. 3. Laboratory-scale forward osmosis device.

3. Results and discussion

3.1. Water quality analysis

Table 4 compares the water quality parameters for feed waters before and after pretreatments. The turbidity of the untreated feed water (wastewater) is 1.29 NTU. After the application of CF, MF, UF, AFM, and AFM with coagulant, the turbidities were reduced to 0.60, 0.01, 0.01, 0.12, and 0.01 NTU, respectively. On the other hand, TOC was not sufficiently removed even after applying the pretreatments and the removal efficiencies were less than 10%. Moreover, the removal efficiency of UV254, which represents the concentration of hydrophobic organic matters, was not high (<10%). These results suggest that the pretreatment methods considered in this study are efficient to remove suspended solids but have limited capability of removing organic matters.

Table 4
Water quality analysis after various pretreatment

	Without pretreatment	Cartridge	MF	UF	AFM	AFM (coagulant)
TOC (mg/L)	5.87	5.76	5.60	5.39	5.40	5.30
TDS (g/L)	4.08	4.09	4.07	4.02	4.08	4.03
UV254 (cm^{-1})	0.208	0.193	0.195	0.183	0.198	0.189
Turbidity (NTU)	1.29	0.60	0.01	0.01	0.12	0.01

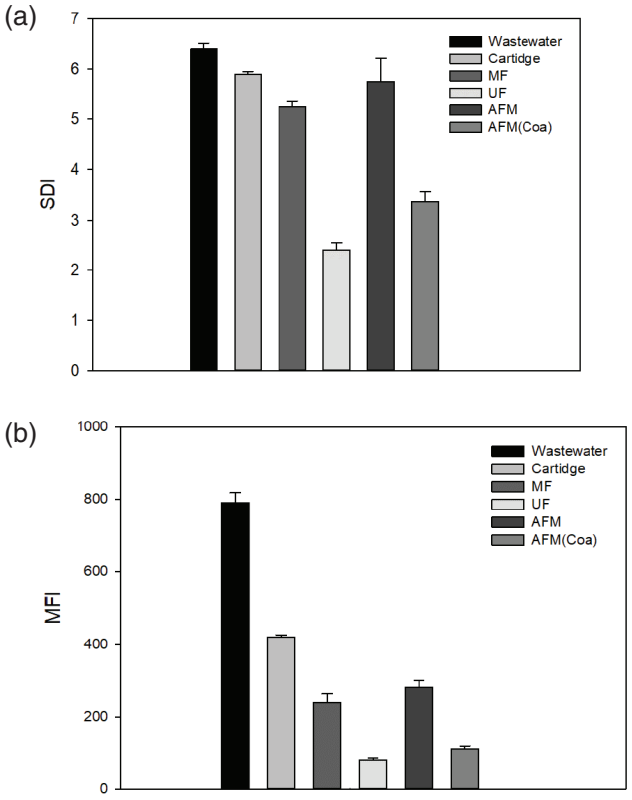

Fig. 4. Comparison of SDI and MFI for different pretreatment methods; (a) SDI and (b) MFI.

3.2. SDI/MFI measurement

The results of SDI and MFI measurements for the pretreatment process are shown in Fig. 4. The untreated wastewater resulted in SDI of 6.4 and MFI of 790 s/L^2. After the pretreatment by the CF and AFM, the SDI was reduced but silt still high. The SDI values were 5.89 and 5.75 for the CF and AFM, respectively. On the other hand, the MFI values substantially decreased after the CF (47%) and after the AFM pretreatment (65%). The SDI and MFI for the MF pretreatment were similar to those for the AFM pretreatment. The UF and AFM with coagulant resulted in lower SDI and MFI values. The SDI values for MF and AFM with coagulant were 2.41 and 3.36, respectively, and the MFI values were 80 and 110 s/L^2, respectively. It is interesting to note that the pretreatment efficiency for the MF was not similar to that for the UF. As shown in Table 5, the apparent water qualities such as TOC, UV254, and turbidity were not much different between the MF and UF pretreatments. Nevertheless, the SDI and MFI for the UF were much lower than those for the MF. The SDI for the UF was 46% of that for the MF and the MFI for the UF was 33% of that for the MF. This suggests that the colloidal materials, which are not measured as TOC, UV254, and turbidity, may significantly affect SDI and MFI values. The measurements were repeated three times for reproducibility and the mean value was used.

Table 5
Summary of SDI and MFI values after pretreatment

	SDI_{15}	MFI_{15} (s/L^2)
Effluent	6.4	790
Cartridge	5.89	420
MF	5.24	240
UF	2.41	80
AFM	5.75	280
AFM (coagulant)	3.36	110

3.3. Changes in FO flux by different pretreatment

Using the pretreated wastewaters, a series of FO experiments were carried out using the two FO membranes. Fig. 5 compares the normalized flux and fouling rate for membrane A. The average initial flux of membrane A was 25 L/m^2h. The FO flux decreases from the beginning when the wastewater was not pretreated. The pretreatments could mitigate flux decline but their effects were not same for different pretreatments. The normalization flux after 20 h of FO operation was 0.84 for the CF, 0.86 for the MF, and 0.91 for the UF. The AFM-only and AFM with coagulant resulted in the final normalized flux of 0.85 and 0.89, respectively.

The experimental results including the normalized flux and fouling rate for membrane B are shown in Fig. 6. The average initial flux of membrane B was 12 L/m^2h, which was lower than that of membrane A. Even if the draw solution was same, membrane B showed a lower flux than membrane A due to its lower water permeability. Nevertheless, the fouling rates for membrane B were higher than those for membrane A.

The overall trends for the effect of pretreatment on flux decline were similar to those in the membrane A. The UF pretreatment resulted in the lowest flux decline and the AFM with coagulant also reduced the flux decline substantially. Except for the untreated wastewater effluent, the feed water pretreated by the CF showed the lowest flux after 20 h of the FO operation. Again, the MF pretreatment was not as effective as the UF pretreatment. The detailed experimental results for membranes A and B are summarized in Table 6.

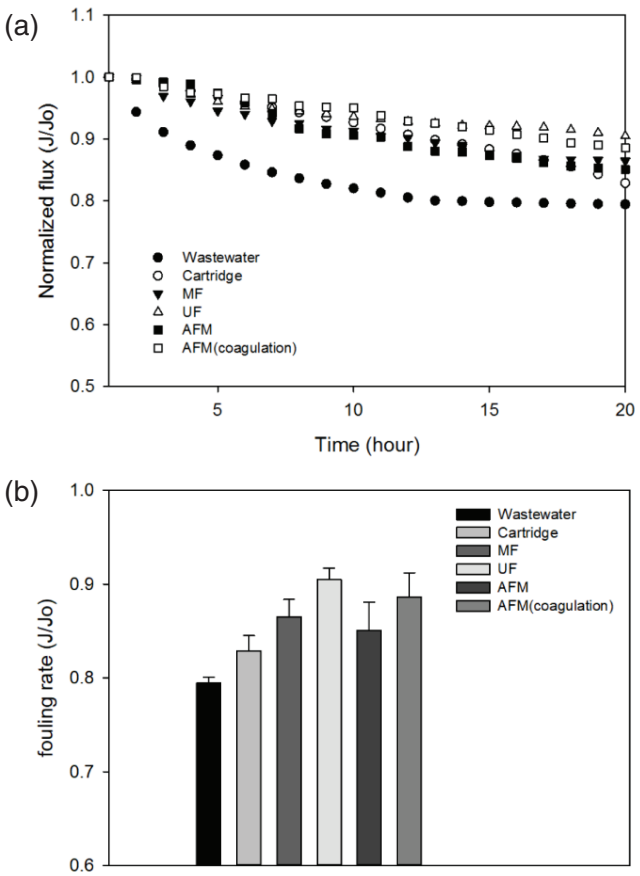

Fig. 5. Graph of (a) change in normalized flux with operating time and (b) final normalized flux after the end of operation for membrane A.

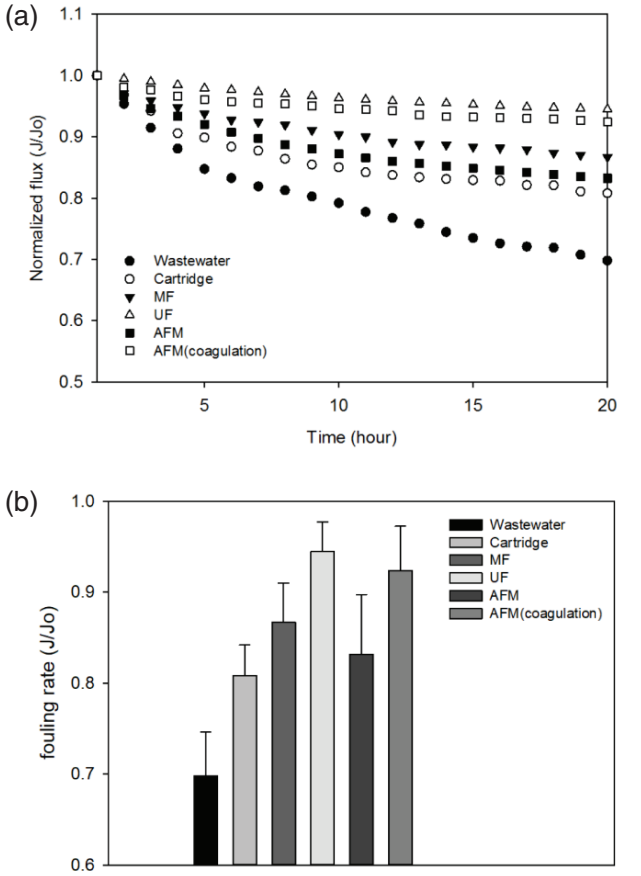

Fig. 6. Graph of (a) change in normalized flux with operating time and (b) final normalized flux after the end of operation for membrane B.

3.4. Analysis of membrane fouling control using FESEM

The surfaces of FO membranes were examined before and after the experiments using a field emission scanning electron microscope (FESEM, S-4700, Hitachi, Japan). Samples were coated with platinum for 2 min before they were taken picture of FESEM. Fig. 7 compares the SEM images of the surfaces of membrane A after the FO experiment. The wastewater effluent without pretreatment led to the formation of thick cake layer on the membrane surface as shown in Fig. 7(f). The use of the CF was not effective to prevent the formation of a foulant layer on the membrane surface as presented by Fig. 7(c). On the other hand, the application of UF and AFM (with coagulant) could effectively prevent foulant layer formation as shown in Figs. 7(a) and (d). Similarly, Figs. 7(b) and (e) show that the formation of the cake layer can be prevented surely than the wastewater effluent without pretreatment but that seems that the effect depends on whether coagulants are used and on the type of pretreatment membrane.

Similar results are shown in the case of membrane B, which are depicted in Fig. 8. Again, the formation of foulant layer was not prevented by the application of the CF while it was controlled by the use of the UF and the AFM with coagulant. These SEM results match with the results of flux decline in Figs. 5 and 6. Accordingly, it is evident that the flux decline in the FO experiments is attributed to the formation of foulant cake layer on the FO membranes. Considering the fact that the turbidity of the MF-treated water is not much different from those of the UF-treated water and the water treated by the AFM with coagulant, it appears that the amount of apparent concentration of suspended solids in the feed water is not closely related to the FO flux decline. Accordingly, it is suggested that the fouling indexes such as SDI or MFI should be used instead of conventional water quality parameters.

Table 6
Summary of normalized flux with different pretreatment process

	Normalized flux	
	Membrane A	Membrane B
Wastewater	0.79	0.63
Cartridge	0.84	0.76
MF	0.86	0.81
UF	0.91	0.90
AFM	0.85	0.74
AFM (coagulant)	0.88	0.86

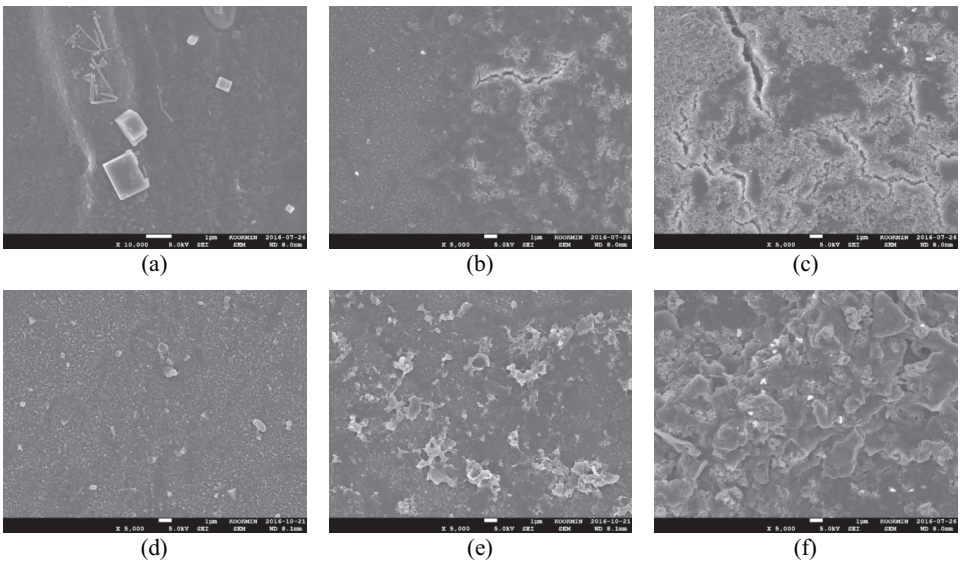

Fig. 7. Comparison of SEM images of membrane A for (a) use of UF, (b) use of MF, (c) use of cartridge filter, (d) use of AFM (coagulant), (e) use of AFM, and (f) without pretreatment.

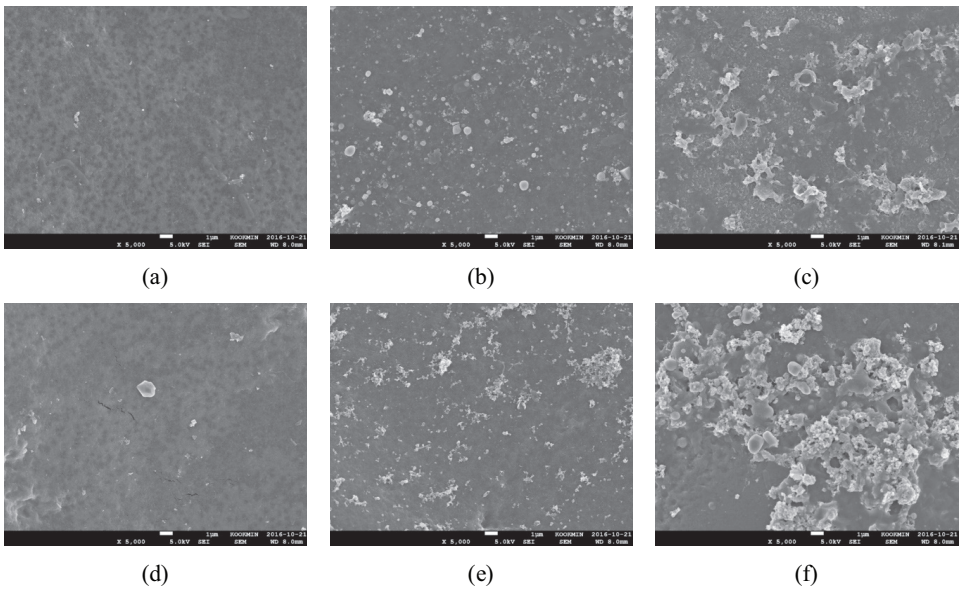

Fig. 8. Comparison of SEM images of membrane B for (a) use of UF, (b) use of MF, (c) use of cartridge filter, (d) use of AFM (coagulant), (e) use of AFM, and (f) without pretreatment.

3.5. Correlation between SDI/MFI and fouling rate

To further investigate the effect of pretreatment on FO fouling, the fouling rates determined by the ratio of flux after the FO experiments to the initial flux (J/J_0) were correlated with the SDI and MFI of the pretreated waters. The results are shown in Fig. 9. Both SDI and MFI showed linear relationships with the fouling rate.

After finishing the experiments, the fouling rates were determined for each membrane system under different pretreatment conditions. The fouling rate depends on the SDI and MFI values and the correlation of MFI is higher than that of SDI. This suggests that SDI and MFI can be used to predict the fouling potential in FO systems. The R^2 values for the regression curves between SDI and fouling rate were 0.8197 for membrane A and 0.8164 for membrane B. As SDI increases, the fouling rate linearly decreases. However, the deviations from the regression curves were significant when the SDI values were close to 6.67. It seems that the SDI measurement for feed waters with high fouling potential is not sensitive enough to quantitatively reflect their fouling potential.

On the other hand, the R^2 values for the regression curves between MFI and fouling rate were 0.926 for membrane A and 0.8997 for membrane B. The R^2 values for MFI were higher

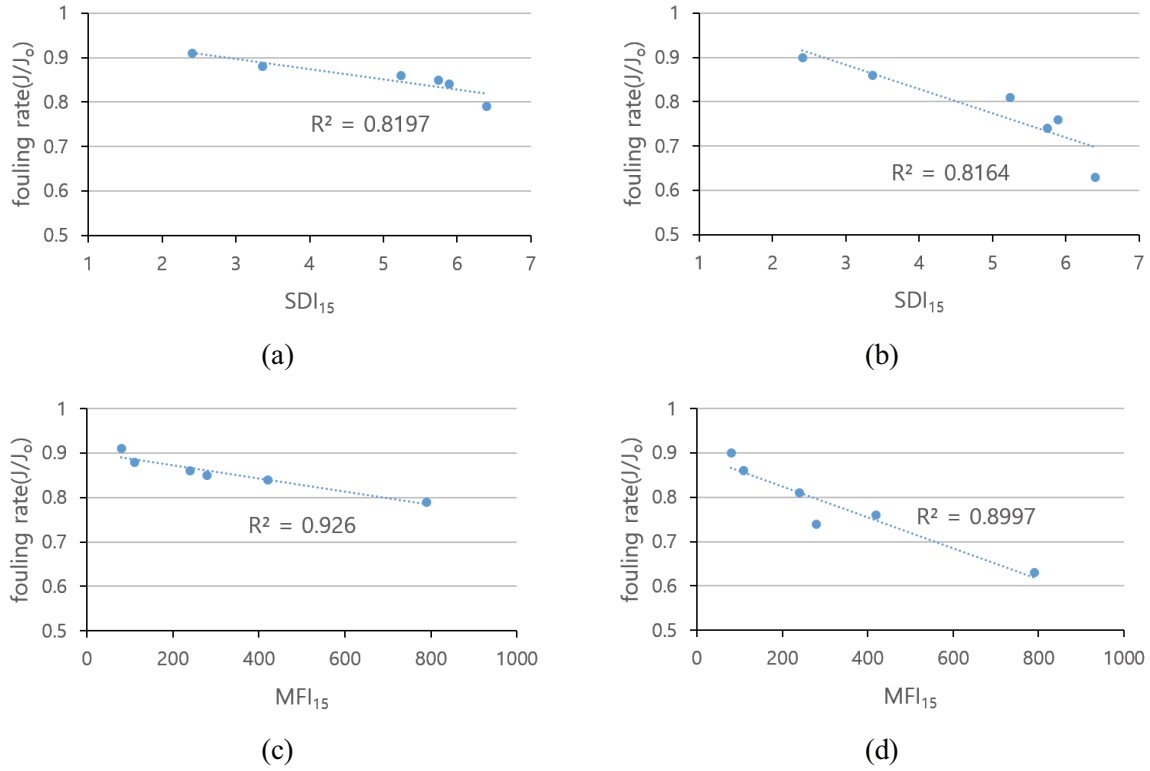

Fig. 9. Correlation curves between SDI/MFI and FO fouling rate. (a) SDI vs. fouling rate for membrane A, (b) SDI vs. fouling rate for membrane B, (c) MFI vs. fouling rate for membrane A, and (d) MFI vs. fouling rate for membrane B.

than those for SDI, indicating that MFI is a better index to predict FO pretreatment efficiency than SDI. Moreover, the deviations from the regression curves were not significant even if the MFI values were high (up to 800 s/L²).

3.6. Application of cake formation model

Hermia's models consist of a standard blocking (SB) model, a complete blocking (CB) model and a cake formation (CF) model, depending on the size of the contaminant. The SB model is a membrane contamination model in which the size of contaminants is so small that the filtration flux is reduced due to the passage of water through the membrane. The CB model is a membrane fouling model in which the size of the pollutant is similar to the size of the pore that is completely blocked by the contaminant, and the porosity is decreased to reduce the filtration flux. The CF model is a membrane fouling model in which the size of contaminants is large and a cake layer is formed on the surface of the membrane to increase the filtration resistance and reduce the filtration flux [26–28].

As shown in Figs. 7 and 8, the formation of cake layer on the FO membrane seems to be the dominant fouling mechanism. Accordingly, the CF model equation was introduced to quantitatively analyze the FO flux decline results. The following model was adopted based on the Hermia's models [26]:

$$J_w = J_{w0}(1+kt)^{-0.5}, \quad \left(\frac{J_{w0}}{J_w}\right)^2 - 1 = kt \tag{4}$$

Table 7
Membrane fouling rate and *R* square for pretreatment process

	Membrane A		Membrane B	
	k	R^2	*K*	R^2
Wastewater	0.040	0.72	0.0786	0.99
CF	0.018	0.96	0.0430	0.87
MF	0.021	0.98	0.0287	0.92
UF	0.012	0.95	0.0134	0.97
AFM	0.021	0.96	0.0469	0.93
AFM (coagulant)	0.014	0.99	0.0208	0.88

Table 7 shows the R^2 values in the model fits of Eq. (4) to the FO experimental data. Overall, the R^2 values were higher than 0.87, confirming that the cake formation is the dominant fouling mechanism of FO membranes in our case. The only exception was the case with untreated wastewater effluent using membrane A, which resulted in the R^2 value of 0.72. It is likely that not only the cake formation but also other fouling mechanisms such as surface blocking were important in this case due to the existence of relatively large suspended solids in the feed water.

The application of the CF model is useful not only for the determination of the fouling mechanisms but also for the estimation and prediction of the fouling propensity [27–28]. Accordingly, Eq. (4) and the *k* values in Table 7 were used to predict the changes in normalized flux of FO with time. The results for membranes A and B are summarized in

Tables 8 and 9, respectively. As expected, the UF and AFM with coagulant are expected to provide the highest flux in both membranes. The order of normalized flux with different pretreatments is as follows:

UF > AFM with coagulant > MF > AFM > CF > untreated wastewater effluent

Fig. 10 compares the correlations between k values from the model fits of the CF model with the SDI and MFI values. Unlike the results in Fig. 9, the k values did not show linear relationships with the SDI values in both FO membranes. The deviations of the experimental data from the regression curves increase with increasing SDI. On the other hand, the k values increase linearly with the MFI values and the R^2 values were relatively high. Accordingly, it is concluded that MFI is more appropriate to predict FO fouling than SDI especially when the fouling potential of the feed water is high.

According to a recent study [30], SDI/MFI as a fouling index was reliable as an index of membrane contamination in RO and PRO process but cake fouling index is proposed to predict RO fouling more accurately than MFI. Thus, the analysis is required that based on CFI considering cake filtration mechanism [31]. However, complex processes require more investment and operational costs and thus, the optimization of pretreatment methods by considering their costs and effectiveness is highly recommended.

Table 8
Prediction of normalized flux of membrane A based on the cake formation model

Time (h)	Wastewater	CF	MF	UF	AFM	AFM (coagulant)
0	1.00	1.00	1.00	1.00	1.00	1.00
10	0.85	0.92	0.91	0.94	0.91	0.94
20	0.75	0.86	0.84	0.9	0.84	0.88
30	0.68	0.8	0.79	0.86	0.78	0.84
40	0.62	0.76	0.74	0.82	0.74	0.8
50	0.58	0.72	0.70	0.79	0.70	0.76
60	0.54	0.69	0.67	0.76	0.67	0.73
70	0.51	0.66	0.64	0.74	0.64	0.71
80	0.49	0.64	0.61	0.71	0.61	0.68

Table 9
Prediction of normalized flux of membrane B based on the cake formation model

Time (h)	Wastewater	CF	MF	UF	AFM	AFM (coagulant)
0	1.00	1.00	1.00	1.00	1.00	1.00
5	0.89	0.93	0.95	0.97	0.92	0.96
10	0.78	0.85	0.89	0.94	0.84	0.92
15	0.67	0.78	0.84	0.91	0.76	0.87
20	0.56	0.70	0.78	0.88	0.68	0.83
25	0.46	0.63	0.73	0.86	0.61	0.79
30	0.35	0.55	0.67	0.83	0.53	0.75
35	0.24	0.48	0.62	0.80	0.45	0.70
40	0.13	0.40	0.56	0.77	0.37	0.66
45	0.02	0.33	0.51	0.74	0.29	0.62
50	–	0.26	0.45	0.71	0.21	0.58

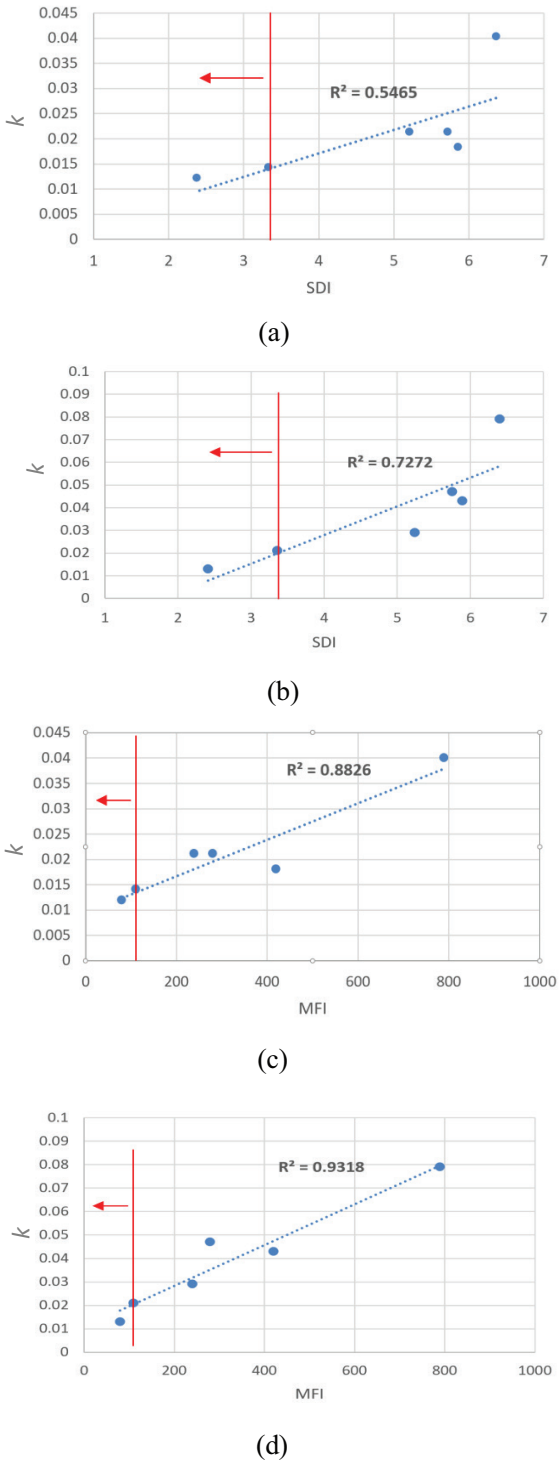

Fig. 10. Correlation curves between SDI/MFI and k values in Table 7. (a) SDI vs. fouling rate for membrane A, (b) SDI vs. fouling rate for membrane B, (c) MFI vs. fouling rate for membrane A and (d) MFI vs. fouling rate for membrane B.

4. Conclusions

In this study, the effect of pretreatment on the FO flux decline was investigated using wastewater effluent as the feed water and real seawater as the draw solution. The following conclusions were drawn:

- The untreated wastewater effluent lead to substantial flux decline after the FO operation of 20 h. This suggests that proper pretreatments are essential. However, pretreatment using the CF was not found to be effective to manage FO flux decline. The best results were obtained by applying the UF or AFM with coagulant. The MF and AFM resulted in moderate pretreatment effects.
- Although the water qualities were similar, different fouling rates were obtained between the MF and UF pretreatment. This indicates that the fouling propensity of the FO membranes was not properly correlated with water quality parameters such as TOC, UV254, and turbidity.
- The correlations between SDI/MFI and FO flux decline were examined. SDI showed reasonable correlation with flux decline ratio (J/J_0) after the FO operation of 20 h but MFI showed better correlations. These results were very similar to evaluation of fouling potential in pressure retarded osmosis applied SDI/MFI [29].
- The results of SEM analysis suggested that the FO flux decline was caused by the cake formation of the foulant on the membrane surface. The model fits using the CF model confirmed this hypothesis. The model parameter k could be predicted by MFI.

Acknowledgments

This subject is supported by Korea Ministry of Environment as “Global Top Project (2016002100001)”.

References

[1] A.D. Khawaji, I.K. Kutubkhanah, J.-M. Wie, Advances in seawater desalination technologies, Desalination, 221 (2008) 47–69.
[2] L.F. Greenlee, D.F. Lawler, B.D. Freeman, B. Marrot, P. Moulin, Reverse osmosis desalination: water sources, technology, and today’s challenges, Water Res., 43 (2009) 2317–2348.
[3] M.A. Shannon, Science and technology for water purification in the coming decades, Nature, 452 (2008) 301–310.
[4] W.L. Ang, A review on the applicability of integrated/hybrid membrane processes in water treatment and desalination plants, Desalination, 363 (2015) 2–18.
[5] R. Lopez-Roldan, Assessment of the water chemical quality improvement based on human health risk indexes: application to a drinking water treatment plant incorporating membrane technologies, Sci. Total Environ., 540 (2016) 334–343.
[6] J. Yin, Polymer-matrix nanocomposite membranes for water treatment, J. Membr. Sci., 479 (2015) 256–275.
[7] M.A. Shannon, P.W. Bohn, M. Elimelech, J.G. Georgiadis, B.J. Marinas, A.M. Mayes, Science and technology for water purification in the coming decades, Nature, 452 (2008) 301–310.
[8] S. Zhao, L. Zou, D. Mulcahy, Brackish water desalination by a hybrid forward osmosis–nanofiltration system using divalent draw solute, Desalination, 284 (2012) 175–181.
[9] B.X. Mi, M. Elimelech, Chemical and physical aspects of organic fouling of forward osmosis membranes, J. Membr. Sci., 320 (2008) 292.
[10] B.X. Mi, M. Elimelech, Gypsum scaling and cleaning in forward osmosis: measurements and mechanisms, Environ. Sci. Technol., 44 (2010) 2022.
[11] L. Robert, M. Elimelech, Global challenges in energy and water supply: the promise of engineered osmosis, Environ. Sci. Technol., 42 (2008) 8625.
[12] J.R. McCutcheon, R.L. McGinnis, M. Elimelech, A novel ammonia–carbon dioxide forward (direct) osmosis desalination process, Desalination, 174 (2005) 1.
[13] Q.C. Ge, J.C. Su, T.S. Chung, G. Amy, Hydrophilic superparamagnetic nanoparticles: synthesis, characterization, and performance in forward osmosis processes, Ind. Eng. Chem. Res., 50 (2011) 382.
[14] J.C. Su, Q. Yang, J.F. Teo, T.S. Chung, Cellulose acetate nanofiltration hollow fiber membranes for forward osmosis processes, J. Membr. Sci., 355 (2010) 36.
[15] N.Y. Yip, A. Tiraferri, W.A. Phillip, J.D. Schiffman, M. Elimelech, High performance thin-film composite forward osmosis membrane, Environ. Sci. Technol., 44 (2010) 3812.
[16] N.Y. Yip, A. Tiraferri, W.A. Phillip, L.A. Hoover, J.D. Schiffman, Y.C. Kim, M. Elimelech, Thin-film composite pressure retarded osmosis membranes for sustainable power generation from salinity gradients, Environ. Sci. Technol., 45 (2011) 4360.
[17] K.L. Lee, R.W. Baker, H.K. Lonsdale, Membranes for power generation by pressure retarded osmosis, J. Membr. Sci., 8 (1981) 141.
[18] R.J. Aaberg, Osmotic power: a new and powerful renewable energy source? Refocus, 4 (2003) 48.
[19] S.E. Skilhagen, J.E. Dugstad, R.J. Aaberg, Osmotic power — power production based on the osmotic pressure difference between waters with varying salt gradients, Desalination, 220 (2008) 476.
[20] M.M. Ling, T.-S. Chung, Desalination process using super hydrophilic nanoparticles via forward osmosis integrated with ultrafiltration regeneration, Desalination, 278 (2011) 194–202.
[21] D. Mosqueda-Jimenez, R.N., T. Matsuura, Membrane fouling test: apparatus evaluation, J. Environ. Eng., 130 (2004) 90–99.
[22] W. Neubrand, S. Vogler, M. Ernst, M. Jekel, Lab and pilot scale investigations on membrane fouling during the ultrafiltration of surface water, Desalination, 250 (2010) 968–972.
[23] M. Habib, U. Habib, A.R. Memon, U. Amin, Z. Karim, A.U. Khan, S. Naveed, S. Ali, Predicting colloidal fouling of tap water by silt density index (SDI): pore blocking in a membrane process, J. Environ. Eng., 1 (2013) 33–37.
[24] S. Lee, S. Kim, J. Cho, E.M.V. Hoek, Natural organic matter fouling due to foulant membrane physicochemical interactions, Desalination, 202 (2007) 377–384.
[25] Y. Ju, I. Hong, S. Hong, Multiple MFI measurements for the evaluation of organic fouling in SWRO desalination, Desalination, 365 (2015) 136–143.
[26] M. Abbasi, A. Taheri, Modeling of permeation flux decline during oily wastewaters treatment by MF-PAC hybrid process using mullite ceramic membranes, Indian J. Chem. Technol., 21 (2014) , 49–55.
[27] E.-E. Chang, S.-Y. Yang, C.-P. Huang, C.-H. Liang, P.-C. Chiang, Assessing the fouling mechanisms of high-pressure nanofiltration membrane using the modified Hermia model and the resistance-in-series model, Sep. Purif. Technol., 79 (2011) 329–336.
[28] Y.-L. Lin, J.-H. Chiou, C.-H. Lee, Effect of silica fouling on the removal of pharmaceuticals and personal care products by nanofiltration and reverse osmosis membranes, J. Hazard. Mater., 277 (2014) 102–109.
[29] Y.K. Choi, S. Vigneswaran, S.H. Lee, Evaluation of fouling potential and power density in pressure retarded osmosis (PRO) by fouling index, Desalination, 389 (2016) 215–223.
[30] N. Quevedo, J. Sanz, A. Lobo, J. Temprano, I. Tejero, Filtration demonstration plant as reverse osmosis pretreatment in an industrial water treatment plant, Desalination, 286 (2012) 49–55.
[31] Y. Jin, Y. Ju, H. Lee, S. Hong, Fouling potential evaluation by cake fouling index: theoretical development, measurements, and its implications for fouling mechanisms, J. Membr. Sci., 490 (2015) 57–64.